Integrated Visualization of Functional and Anatomic Brain Data: A Validation Study

Rik Stokking, Johannes W. van Isselt, Peter P. van Rijk, John M.H. de Klerk, Antoon W.L.C. Huiskes, Ilse J.R. Mertens, Erik Buskens and Max A.Viergever

Image Sciences Institute, Utrecht University, University Hospital, Utrecht, The Netherlands

Two-dimensional SPECT display and three methods for integrated visualization of SPECT and MRI patient data are evaluated in a multiobserver study to determine whether localization of functional data can be improved by adding anatomical information to the display. **Methods:** SPECT and MRI data of 30 patients were gathered and presented using four types of display: one of SPECT in isolation, two integrated two-dimensional displays and one integrated three-dimensional display. Cold and hot spots in the peripheral cortex were preselected and indicated on black-and-white hard copies of the image data. Nuclear medicine physicians were asked to assign the corresponding spots in the image data on the computer screen to a lobe and a gyrus and give a confidence rating for both localizations. Interobserver agreement using kappa statistics and average confidence ratings were assessed to interpret the reported observations. **Results:** Both the interobserver agreement and the confidence of the observers were greater for the integrated two-dimensional displays than for the two-dimensional SPECT display. An additional increase in agreement and confidence was seen with the integrated three-dimensional display. **Conclusion:** Integrated display of SPECT and MR brain images provides better localization of cerebral blood perfusion abnormalities in the peripheral cortex in relation to the anatomy of the brain than single-modality display and increases the confidence of the observer.

Key Words: validation; integrated visualization; multimodality imaging; SPECT; MRI

J Nucl Med 1999; 40:311–316

Integrated visualization is aimed at the efficient presentation of information from different sources, usually combining a functional modality (SPECT, PET, functional MRI) with an anatomic modality (CT, MRI). Correlation of functional processes with anatomical structures is hampered by the low spatial resolution of functional imaging modalities (*1–3*). These modalities might benefit from additional anatomical information provided by MRI and/or CT (*4–8*). In previous articles (*9,10*), several techniques have been proposed for integrated visualization of functional and anatomic brain images. This article presents a multiple-observer study to evaluate three of these techniques, two for two-dimensional and one for three-dimensional display, to determine whether integrated visualization improves diagnostic agreement. The diagnostic task for this study is the localization of cold and hot spots in the peripheral cortex. We focus on the fusion of ^{99m}Tc-hexamethyl propyleneamine oxime (HMPAO)-SPECT and T1-weighted three-dimensional gradient-echo MRI of the brain.

Received Feb. 2, 1998; revision accepted Jun. 4, 1998.

For correspondence or reprints contact: Rik Stokking, PhD, Diagnostic Radiology, 333 Cedar St., 332 BML, PO Box 208042, Yale University, New Haven, CT 06520-8042.

INTEGRATED TWO-DIMENSIONAL VISUALIZATION

Adjacent displays of two-dimensional images from different sources on a lightbox or a computer monitor can be considered the most rudimentary form of integrated visualization. A valuable extension of this approach is the use of a linked cursor indicating corresponding locations in several images (*11*). Integration of information from two or more image slices into one two-dimensional image has been performed using alternate pixel display, color integration procedures, additional dimensions (e.g., height or time) and areas and contours (*7,9,11–14*). Two categories can be distinguished: (a) nonselective integration, in which all information from the images, whether relevant or not, is combined using techniques such as multiplication, addition or color scaling; and (b) selective integration, in which specific diagnostic features (e.g., regions, object boundaries, intensity ranges) are extracted and subsequently integrated into the display of another modality with the objective to convey only the relevant information required to perform the diagnostic task. Nonselective integration of SPECT and MRI data conveys little if any more information than adjacent display. Moreover, valuable features may be camouflaged by nondiagnostic information (*9*). Consequently, although these techniques are easy to use and allow fast visualization, they are not effective. Color models, especially hue saturation value (HSV) (*9*), hold more promise, because the human visual system uses color more effectively than gray levels (*15*).

Selective integration of SPECT and MRI data allows a more effective display of the relevant information. Initially the cost of segmentation was the main drawback, but in the past few years semi- or fully automated segmentation methods to extract the brain from T1-weighted MR images have become available (*16–18*).

INTEGRATED THREE-DIMENSIONAL VISUALIZATION

Integrated three-dimensional visualization of functional and anatomical brain data includes windows (*4,9,19*), cut-

planes (*9, 20*), opacity-weighted display (*20*) and surface-mapping methods (*4,10,19,21*). Furthermore, an integrated three-dimensional presentation can be focused on the visualization of already-detected abnormalities (*20,22*), so that standard volume visualization methods can be applied (*23*).

In previous work, we experimented with several of these techniques and found the normal fusion approach, especially, to be promising (*10*). A preliminary clinical evaluation of the normal fusion technique was conducted, which indicated that anatomic localization and communication might benefit from this technique. It was concluded that a thorough evaluation was required to establish whether simultaneous display of SPECT and MRI indeed offers increased diagnostic agreement among raters. In this study, we investigate the value of additional anatomic information for the localization of functional processes in patient brain data.

MATERIALS AND METHODS

Patient Data

Patient material was gathered by listing all patients with appropriate ^{99m}Tc-HMPAO SPECT and T1-weighted three-dimensional gradient-echo MRI brain scans. The principal author (not a rater) selected from this list a total of 30 patient datasets. Absence of gross abnormalities in both SPECT and MRI data were used as the selection criterion. All 30 cases were acquired under the instruction of the Department of Child Psychiatry (average age: 11 y with SD of 3 y). Tourette's syndrome and/or attention deficit hyperactivity disorder and/or comorbid disorders were diagnosed in most of the patients. Autistic behavior or obsessive compulsive disorder was diagnosed in the remaining patients. Nuclear medicine physicians were supplied with only the image data; no information concerning the patients could be consulted. T1-weighted three-dimensional gradient-echo MR images were acquired with a whole-body Philips Gyroscan 0.5-T (Best, The Netherlands) using a standard head coil. The acquisition data of the whole head consisted of contiguous axial slices of 1.2-mm thickness with a repetition time of 30 ms, an echo time of 13 ms, 256 × 256 matrix and a 230 mm field of view. SPECT image data were acquired with a Picker PRISM three-detector with three-head gamma camera (Picker International, Cleveland Heights, OH) using a long-bore ultra-high-resolution, low-energy fanbeam collimator and reconstructed to contiguous axial slices with a 64 × 64 matrix, a slice thickness of approximately 7.1 mm and a plane resolution of 7.5 mm full width at half maximum.

Three additional cases were used in a training session before this localization study to familiarize observers with the setup and anatomic information. These cases had been used in a previous study (*10*) and three of the five observers had worked with these training data at that time. Two of these cases were highly comparable to the 30 patient datasets. The third dataset was different (adult with a frontal lobe asterocytoma), but this was not considered relevant for the training session.

Registration and Segmentation

Prerequisites for integrated visualization are (a) adequate registration of the modalities whereby the transformation matrix is calculated to relate the coordinate systems of different datasets (*24*), and (b) accurate segmentation to indicate interesting structures to be visualized (*17,25*).

The registration was performed using the mutual information technique (*26*). This automatic, robust, retrospective registration technique maximizes the statistical dependence between image intensities of voxel pairs of different datasets, thereby calculating the required transformation matrix to align them geometrically. The resulting matrix was applied to the SPECT data using cubic convolution (*27*), in effect resampling the SPECT data to the MRI data.

Segmentation of an MRI dataset was performed in 15 min using ANALYZE (BIR-Mayo Clinic, Rochester, MN) (*16*), based on region growing and mathematical morphology as described in Hohne and Hanson (*28*). The segmented brain was used for the three-dimensional normal fusion visualizations and for defining the outer brain contours in transverse MRI slices. These contours were subsequently superimposed onto the corresponding registered SPECT images for integrated two-dimensional display.

Display Methodology

We evaluated the value of integrated visualization as opposed to single-modality SPECT display. The basis for the latter is the routine viewing of SPECT data in the nuclear medicine department, supported by the reporting and image manipulation program MedView (MedImage Inc., Ann Arbor, MI). Multiplanar two-dimensional images can be displayed along the three orthogonal axes of the volume data and a cross-hair can be used to determine the three-dimensional position of a given location. A mouse click in one of the images updates the other orthogonal images to the indicated position. In addition, a color lookup table can be chosen and changed at will by the observer. This program was used for all two-dimensional images to ensure viewing conditions identical to those in the clinical situation.

Three integrated visualization techniques were used for the validation study: (a) integrated two-dimensional visualization with adjacent display (denoted as two-dimensional adjacent); (b) integrated two-dimensional visualization with selective integration of contours of the brain from MRI superimposed onto the SPECT data (denoted as two-dimensional contour); and (c) integrated three-dimensional visualization using images rendered with the normal fusion technique of the SPECT/MRI data (in this article denoted as three-dimensional normal fusion). The visualization techniques in this validation study have been described in previous reports and will be reviewed only briefly here.

For the contours from the MRI data superimposed onto the SPECT images, we used a value corresponding to the maximum SPECT value, in effect assigning the highest lookup table color (usually white) to the contours. With the normal fusion technique, local functional information is sampled and projected onto an anatomic structure along a path defined by the inward normal of the local surface direction (*9,10*). In this study, the SPECT data below the cortical surface were sampled in the range of 0–15 mm. The average value was subsequently color encoded onto the MRI cortex rendering, so as to signal both cold and hot spots. Observers were supplied with one image containing six orthogonal normal fusion visualizations of the brain under investigation (Fig. 1D). The color encoding of the SPECT data in the three-dimensional integrated display could be easily manipulated with a technique described in Stokking (*18*). However, this was not supported by MedView, and

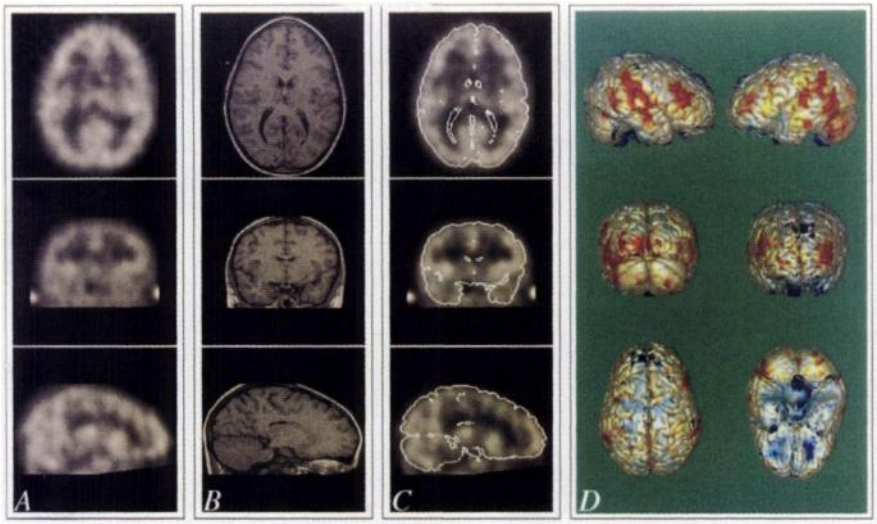

FIGURE 1. Three integrated displays used for validation of the localization task. Two-dimensional images of datasets could be investigated with three orthogonal views (coronal, sagittal and transversal) and a cross-hair could be used to determine location of a given point. (A and B) Two-dimensional adjacent display of (registered) SPECT images and corresponding MR slices are shown. (C) Two-dimensional contour display. (D) Three-dimensional normal fusion images show renderings from six orthogonal directions.

another system was used so that special care could be taken to ensure viewing conditions similar to the clinical situation.

Setup

The task for this validation study was to localize functional spots in the peripheral cerebral cortex of patient image data using four display types (Fig. 1). Focal hot and cold spots were preselected by the principal author (not a rater) based on their distinctive presence in all display types. The location of the indicated spots was verified to be identical in all display types. The localization task was performed by five nuclear medicine physicians in their usual setting. Cases were randomized for each display type. Complete randomization over all display types was impractical, because raters would have to switch between different displays and monitors. In addition, an undesirable memory effect would have been introduced, since experience from the training session showed that the three-dimensional normal fusion images made certain spots easier to remember. The incomplete randomization may introduce a learning effect, but this should be minimized by the training session.

Localization was restricted to cold and hot spots in the peripheral cerebral cortex. The three-dimensional normal fusion method is not suitable for the presentation of functional information in other parts of the brain. To avoid ambiguities in the localization of patient data, only focal spots were used. (Spots that span an area may cause problems in assignment to a specific lobe or gyrus.) A total of 122 spots resulted in 122 × 5 raters × 4 displays = 2440 observations, consisting of a lobe and gyrus localization and a confidence rating for both. The location of a cortical spot had to be assigned to a lobe (frontal, parietal, occipital or temporal) and gyrus (e.g., superior temporal gyrus). The observers were supplied with atlases (*29–31*) for reference on brain anatomy and a schematic summary (Fig. 2). Both localization aspects were rated with a confidence measure ranked: 1 = very confident, 2 = confident, 3 = reasonably confident, 4 = low confidence and 5 = no confidence. Statistical evaluation was performed using a kappa (κ) value for interobserver variability on localization and an average value for confidence.

The spots to be localized with the two-dimensional displays were indicated on paper copies of the image data for the two-dimensional displays (for the two-dimensional adjacent and two-dimensional contour displays, registered SPECT images were used) and on (black-and-white) paper copies of the six normal fusion visualizations for the three-dimensional display. The spots to be localized were indicated on the hard copies with a superimposed circle and code that consisted of a C for cold spots, an H for hot spots and a number (Fig. 3). Raters localized corresponding spots in the image data on screen for all four display types.

Statistical Analysis

Interobserver agreement for more than two raters can be assessed using the κ value proposed by Fleiss (*32*), which represents agreement corrected for chance agreement. Other measures were also considered (e.g., the interclass correlation coefficient), but the κ value was preferred because our data were nonordered categorical. Furthermore, κ statistics correct for chance agreement, which facilitates clinical interpretation. Landis and Koch (*33*) ranked the κ value as follows: less than 0.00, poor agreement; 0.00–0.20, slight agreement; 0.21–0.40, fair agreement;

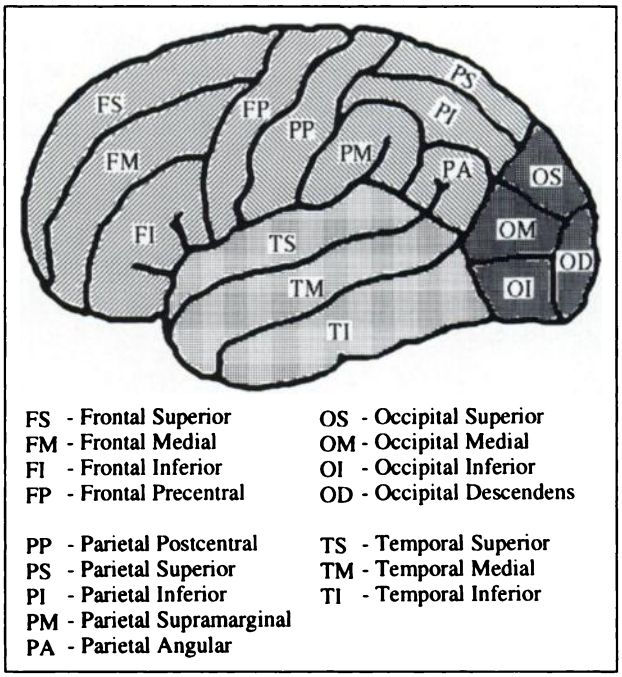

FIGURE 2. Schematic subdivision of brain in lobes and gyri for localization of abnormalities.

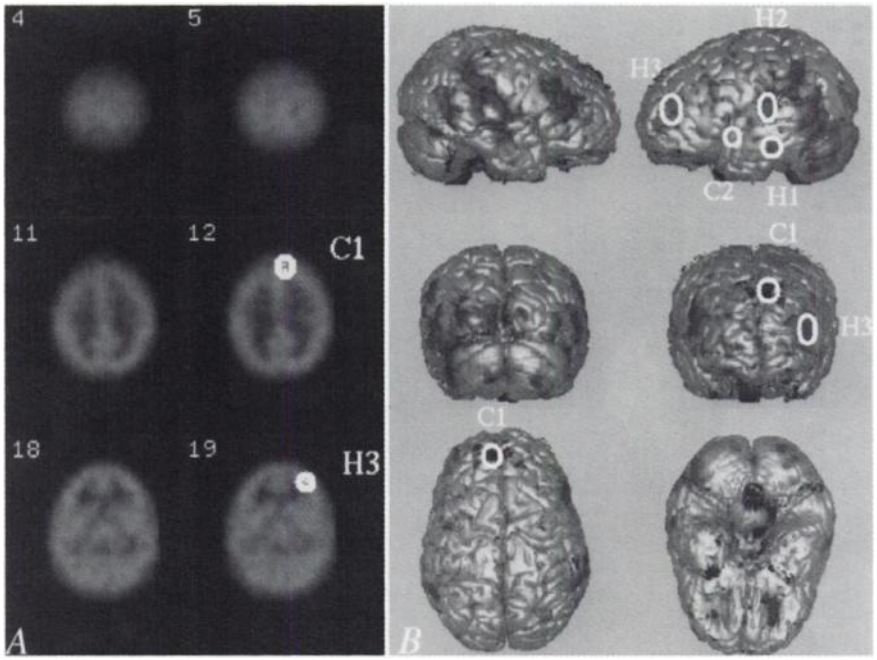

FIGURE 3. Selection of printed images used to indicate preselected cold (C1 and C2) and hot spots (H1, H2 and H3) to be localized. (A) Sample images of two-dimensional display. (B) Sample of three-dimensional display.

0.41–0.60, moderate agreement; 0.61–0.80, substantial agreement; and 0.81–1.00, almost perfect agreement.

$$\kappa = \frac{\sum_{a=1}^{n}\sum_{\substack{b=1 \\ b\neq a}}^{n}(1 - P_{a,b})\kappa_{a,b}}{\sum_{a=1}^{n}\sum_{\substack{b=1 \\ b\neq a}}^{n}(1 - P_{a,b})} \quad with: \quad \kappa_{a,b} = \frac{P_i - P_{a,b}}{1 - P_{a,b}} \quad \text{Eq. 1}$$

$$95\%\ CI = \kappa \pm 1.96 * sd_{\kappa}$$

Equation 1 expresses the κ value over all observers, which is a weighted average of the κ values over all observer pairs $\kappa_{a,b}$. $P_{a,b}$ is the expected proportion of agreement between the ath and the bth observer under the null hypothesis of independence, i.e., chance agreement. P_i is the observed proportion of agreement between two observers. The 95% confidence interval (CI) is calculated from the SD over all $\kappa_{a,b}$ calculations. For details we refer to Fleiss (*32*). The κ values and 95% CI were calculated using Agree 5.0 for computing agreement on nominal data (R. Popping, iecProGamma, The Netherlands). The confidence ratings for the lobar and gyral localization for each of the four display types were calculated using an arithmetic mean over all observations.

RESULTS

In Table 1 the final results over all measurements are presented for each of the display types. The first row presents the results for the two-dimensional SPECT display; row 2, the two-dimensional adjacent display; row 3, the two-dimensional contour display; and row 4, the three-dimensional normal fusion display. The columns are divided into two parts, lobes and gyri, for anatomic localization. Each localization part is subdivided into a κ value with 95% CI and an average measure of perceived confidence in the localization given.

The results show that the κ value measuring observer agreement for localization increases when anatomic data from MRI is added to the SPECT information. There is no significant statistical difference between the two-dimensional adjacent and two-dimensional contour displays, but, for gyral localizations, the three-dimensional normal fusion display is superior to both integrated two-dimensional displays. The average confidence measure shows similar results, i.e., the confidence of the observers in their localizations increases when additional anatomic information is supplied. Again, the three-dimensional normal fusion display improves observer confidence for gyral localizations.

TABLE 1
Results for Lobar and Gyral Localization of Cold and Hot Spots

	Lobe		Gyrus	
	κ ± 95% CI	Confidence	κ ± 95% CI	Confidence
Two-dimensional SPECT	0.74 ± 0.03	1.6	0.32 ± 0.02	2.8
Two-dimensional adjacent	0.84 ± 0.03	1.3	0.40 ± 0.02	2.4
Two-dimensional contour	0.84 ± 0.03	1.3	0.38 ± 0.02	2.4
Three-dimensional normal fusion	0.86 ± 0.03	1.2	0.54 ± 0.02	2.0

Interobserver correspondence is expressed as a κ value with 95% confidence interval (CI), and an average confidence measure is calculated for the four display settings.

DISCUSSION

The κ and confidence values for lobar localizations are very high, which signifies a high accuracy for this task even for two-dimensional SPECT display. Additional anatomical information from the integrated two-dimensional displays improves the interobserver agreement and confidence of observations. A significant further improvement cannot be accomplished using three-dimensional normal fusion. This suggests that the two-dimensional contour and two-dimensional adjacent displays are sufficiently accurate for lobar localization. However, all observers noted that localization was performed considerably faster with the three-dimensional normal fusion display.

Because of the relatively low spatial resolution, gyral localization of spots in SPECT images is more difficult than lobar localization, which explains the lower κ and confidence values. For this task, the three-dimensional normal fusion display outperforms the other techniques appreciably and has a κ value with acceptable accuracy.

Overall, the observers reported a strong appreciation for additional anatomic information, which they do not usually have available on screen. The normal fusion images, especially, were appreciated as a pleasant and fast method for localizing abnormalities. Some of the observers reported a preference for the two-dimensional adjacent display over the two-dimensional contour display, because the contours were considered annoying because they interfered with the SPECT data. However, the results indicate that the two-dimensional contour display is as effective as the two-dimensional adjacent display for localization of spots. Furthermore, the adjacent display of images still requires mental integration by the observer. The addition of a linked cursor is helpful, but integrated images appear to alleviate overall screening even more. Also, the two-dimensional adjacent display causes problems in color assignment on an 8-bit color display and approximately doubles computer memory requirements compared with two-dimensional contour display. We consider the two-dimensional contour display to be at least as promising for integrated two-dimensional display as adjacent display. An additional option to turn the contour on and off is expected to resolve the initial criticism.

Two more general considerations are offered: (a) Findings in a young patient group may not have a direct relationship to adult patients in all circumstances. However, we consider the age of our sample (<21 y) of little or no influence for this particular study. (b) Localization, not detection, of functional abnormalities is evaluated. The latter remains to be investigated and probably requires the simulation of SPECT data from MR image data.

CONCLUSION

Fusion of SPECT and MRI information increases the ability of clinicians to localize spots in the functional SPECT data of the peripheral cortex and increases confidence in their observations. Volumetric display using the normal fusion technique has proven particularly efficient for this purpose. The results indicate that detected abnormalities present in SPECT data can be localized with acceptable accuracy at the gyral level by supplying additional anatomic information. This finding opens up new possibilities for clinical procedures in which precise localization of functional information is required.

ACKNOWLEDGMENTS

This research was performed within the framework of the research program "Imaging Science," cosponsored by Philips Medical Systems, KEMA, Shell International Exploration and Production and ADAC Europe. We are indebted to our colleagues P.C. Anema, F.J. Beekman, B. Derksen, R.T.M. Jonk, C. Haring, R.M. Hoogeveen, J. Kervel, J.B.A. Maintz and L.C. Meiners. We gratefully acknowledge the research licence of ANALYZE, provided by Dr. R.A. Robb, Mayo Foundation/Clinic, Rochester, MN.

REFERENCES

1. Evans AC, Marrett S, Torrescorzo J, Ku S, Collins L. MRI-PET correlation in three dimensions using a volume-of-interest (VOI) atlas. *J Cereb Blood Flow Metab.* 1991;11:A69–A78.
2. Kundel HL. Visual cues in the interpretation of medical images. *J Clin Neurophysiol.* 1990;7:472–483.
3. Zubal GI, Spencer SS, Imam K, et al. Difference images calculated from ictal and interictal technetium-99m-HMPAO SPECT scans of epilepsy. *J Nucl Med.* 1995;36:684–689.
4. Levin DN, Hu X, Tan KK, et al. The brain: integrated three-dimensional display of MR and PET images. *Radiology.* 1989;172:783–789.
5. Holman BL, Zimmerman RE, Johnson KA, et al. Computer assisted superimposition of magnetic resonance and high-resolution technetium-99m-HMPAO and thallium-201 SPECT images of the brain. *J Nucl Med.* 1991;32:1478–1485.
6. Valentino DJ, Mazziotta JC, Huang H. Volume rendering of multimodal images: Application to MRI and PET imaging of the human brain. *IEEE Med Imaging.* 1991;10:554–562.
7. Viergever MA, van den Elsen PA, Stokking R. Integrated presentation of multimodal brain images. *Brain Topogr.* 1992;5:135–145.
8. Britton K. Highlights of the annual meeting of the European Association of Nuclear Medicine, Lausanne 1994. *Eur J Nucl Med.* 1994;21:159–169.
9. Stokking R, Zuiderveld KJ, Hulshoff Pol HE, Viergever MA. Integrated visualization of SPECT and MR images for frontal lobe damaged regions. In: Robb RA, ed. *Visualization in Biomedical Computing 1994.* Proc. SPIE, Vol. 2359. Bellingham, WA: SPIE Press; 1994:282–290.
10. Stokking R, Zuiderveld KJ, Hulshoff Pol HE, van Rijk PP, Viergever MA. Normal fusion for 3D integrated visualization of SPECT and MR brain images. *J Nucl Med.* 1997;38:624–629.
11. Hawkes DJ, Hill DLG, Lehmann ED, Robinson GP, Maisey MN, Colchester ACF. Preliminary work on the interpretation of SPECT images with the aid of registered MR images and an MR derived 3D neuroanatomical atlas. In: Hohne KH, Fuchs H, Pizer S, eds. *3D Imaging in Medicine.* Berlin, Germany: Springer-Verlag; 1990:242–251.
12. Weiss KL, Stiving SO, Herderick EE, Cornhill JF, Chakeres DW. Hybrid color MR imaging display. *AJR.* 1987;149:825–829.
13. Pelizzari CA, Chen GTY, Spelbring DR, Weichselbaum RR, Chen CT. Accurate three-dimensional registration of CT, PET, and/or MR images of the brain. *J Comput Assist Tomogr.* 1989;13:20–26.
14. Condon BR. Multi-modality image combination: Five techniques for simultaneous MR-SPECT display. *Comput Med Imaging Graph.* 1991;15:311–318.
15. Alfano B, Brunetti A, Ciarmiello A, Salvatore M. Simultaneous display of multiple MR parameters with quantitative magnetic color imaging. *J Comput Assist Tomogr.* 1992;16:634–640.
16. Robb RA, Hanson DP. The ANALYZE software system for visualization and analysis in surgery stimulation. In: Taylor RH, Lavallee S, Burdea GC, Mosges R, eds. *Computer-Integrated Surgery.* Cambridge, MA: MIT Press; 1996:175–189.

17. Niessen WJ. *Multiscale Medical Image Analysis* [PhD thesis]. Utrecht, The Netherlands: Utrecht University; 1997.
18. Stokking R. *Integrated Visualization of Functional and Anatomical Brain Images* [PhD thesis]. Utrecht, The Netherlands: Utrecht University; 1998.
19. Hu X, Tan KK, Levin DN, Pelizzari CA, Chen GT. A volume-rendering technique for integrated three-dimensional display of MR and PET data. In: Hohne KH, Fuchs H, Pizer S, eds. *3D Imaging in Medicine*. Berlin, Germany: Springer-Verlag; 1990:379–397.
20. Evans AC. Correlative analysis of three-dimensional brain images. In: Taylor RH, Lavallee S, Burdea GC, Mosges R, eds. *Computer-Integrated Surgery*. Cambridge, MA: MIT Press; 1996:99–114.
21. Payne BA, Toga AW. Surface mapping brain function on 3D models. *IEEE Comput Graph*. 1990;10:33–41.
22. Wowra B, Schad L, Schlegel W, Kunze S. Scopes of computer application in stereotactic neurosurgery. In: Lemke HU, Rhodes M, Jaffe C, Felix R, eds. *Computer Assisted Radiology '89*. Berlin, Germany: Springer-Verlag; 1989:296–301.
23. Wallis JW. Three-dimensional display in SPECT imaging: Principles and applications. In: Reiber JHC, van der Wall EE, eds. *Cardiovascular Nuclear Medicine and MRI*. Dordrecht, The Netherlands: Kluwer Academic Publishers; 1992: 89–100.
24. Maintz JBA, Viergever MA. A survey of medical image registration. *Med Image Anal*. 1998;2:1–36.
25. Clarke LP, Velthuizen RP, Camacho MA, et al. MRI segmentation: methods and applications. *Magn Reson Imaging*. 1995;13:343–368.
26. Maes F, Collignon A, Vandermeulen D, Marchal G, Suetens P. Multimodality image registration by maximization of mutual information. *IEEE Med Imaging*. 1997;16:187–198.
27. Parker J, Kenyon R, Troxel D. Comparison of interpolating methods for image resampling. *IEEE Med Imaging*. 1983;MI-2:31–39.
28. Hohne KH, Hanson WH. Interactive 3D segmentation of MRI and CT volumes using morphological operations. *J Comput Assist Tomogr*. 1992;16:285–294.
29. Duvernoy HM. *The Human Brain: Surface, Three-Dimensional Sectional Anatomy and MRI*. Vienna, Austria: Springer-Verlag; 1991.
30. Kahle W, Leonhardt H, Platzer W. *Atlas der Anatomie* [Dutch translation]. 12th ed. Munich, Germany: Deutscher Taschenbuch Verlag; 1995.
31. Gray H. *Gray's Anatomy*. 16th ed. Pick TP, Howden R, eds. London, England: Senate Studio Editions Ltd.; 1994;809–819.
32. Fleiss JL. Measuring nominal scale agreement among many raters. *Psychol Bull*. 1971;76:378–383.
33. Landis RJ, Koch GG. The measurement of observer agreement for categorical data. *Biometrics*. 1977;33:159–174.